Conical Defects in Growing Sheets

Martin Michael Müller and Martine Ben Amar
Laboratoire de Physique Statistique de l'Ecole Normale Supérieure (UMR 8550), associé aux Universités Paris 6 et Paris 7 et au CNRS; 24, rue Lhomond, 75005 Paris, France

Jemal Guven
Instituto de Ciencias Nucleares, Universidad Nacional Autónoma de México, Apdo. Postal 70-543, 04510 México D.F., Mexico
(Received 7 July 2008; published 10 October 2008)

A growing or shrinking disc will adopt a conical shape, its intrinsic geometry characterized by a surplus angle φ_e at the apex. If growth is slow, the cone will find its equilibrium. Whereas this is trivial if $\varphi_e \leq 0$, the disc can fold into one of a discrete infinite number of states if $\varphi_e > 0$. We construct these states in the regime where bending dominates and determine their energies and how stress is distributed in them. For each state a critical value of φ_e is identified beyond which the cone touches itself. Before this occurs, all states are stable; the ground state has twofold symmetry.

DOI: 10.1103/PhysRevLett.101.156104 PACS numbers: 68.55.−a, 02.40.Hw, 46.32.+x

Soft matter systems may display enormous complexity at the microscopic level [1,2]. However, on mesoscopic or larger scales of physical interest, the relevant degrees of freedom very often turn out to be purely geometrical. If one dimension is much smaller than the two others, an effective description in terms of a two-dimensional surface becomes appropriate. This is just as true for biological membranes [3,4] as it is for inanimate matter [5].

The equilibrium shape of the surface is often a minimum of bending energy. Typically however, one must take into account external forces, or constraints on the geometry: these may be *global* as in the fluid membranes occurring in cells in which the area or the enclosed volume is fixed; they may also be *local* as in plant tissues which are described, to a good approximation, as an unstretchable surface with a fixed metric [6,7].

In general, bending is not possible without stretching. It turns out, however, that the most effective way to minimize the energy and satisfy the constraint is by confining the regions where stretching occurs to a series of sharp peaks and ridges [8,9]. On length scales much larger than the thickness of the sheet, these can then be treated as points and curves along which boundary conditions are set on the surface. The simplest geometry of this kind is the developable cone—the ''point defect'' of folding, with the bending energy localized near the apex. Such a geometry is illustrated beautifully by a flat planar disc of paper depressed into a circular frame by applying a point force to its center [10].

Conical shapes also occur in living tissues. The unicellular algae *Acetabularia acetabulum*, for example, grows a conical cap in the course of its development [7,11]. Despite the superficial similarity, however, the pointlike singularity exhibited in such cones is very different from the one which appears in the developable cone. In the latter, the singularity at the apex is extrinsic; the metric itself remains the same as that of the original disc. This is captured by the fact that the surplus angle at the apex vanishes: the length of the closed curve at a unit distance from the apex is equal to 2π. If, however, there is a surplus or a deficit, there will be a nontrivial folded state even when external forces do not act. Whereas this state is an unremarkable circular cone in the case of a deficit, when the deficit is turned to surplus, the folded shape—an *excess* cone (e cone for short)—exhibits a surprisingly subtle behavior. In this Letter, we will describe the equilibrium states associated with these ''point defects'' in the full nonlinear theory. Remarkably, there exists a discrete infinity of states (they are ''quantized''); they can therefore be completely classified in terms of the surplus angle φ_e and a quantum number n. For each n we show that there is a critical value of φ_e, increasing monotonically with n, beyond which the cone makes contact with itself; if $\varphi_e > 35.23$ self-contact cannot be avoided. The resulting shapes are not unlike the collars—called ruffs—one associates with portraits by Rembrandt or Hals.

To understand the physics of e cones we identify the stresses which underpin their geometry. We also address the question of stability. What is the ground state? Are all equilibria local minima of the bending energy? To answer these questions, one must take care not to lose sight of the local constraint of isometry. It is reassuring that one can easily build paper models and put the results of this analysis to the test.

Geometry and energy.—The e cone can be parametrized in terms of a closed curve Γ: $s \rightarrow \boldsymbol{u}(s)$ on the unit sphere where the arclength s runs from 0 to $s_e = 2\pi + \varphi_e$ along this curve (see Fig. 1). If r denotes the radial distance from the origin, the surface is described by the vector function $\boldsymbol{X}(r, s) = r\boldsymbol{u}(s)$. Its direction in Euclidean space $\mathbb{R}^3$ will be given by the polar and azimuthal angles on the sphere, φ and ϑ, respectively. The tangent vectors to the e cone are $\boldsymbol{u}$ and $\boldsymbol{t} = \boldsymbol{u}'$ where the prime denotes a derivative with respect to s. Together with the normal $\boldsymbol{n} = \boldsymbol{u} \times \boldsymbol{t}$ these

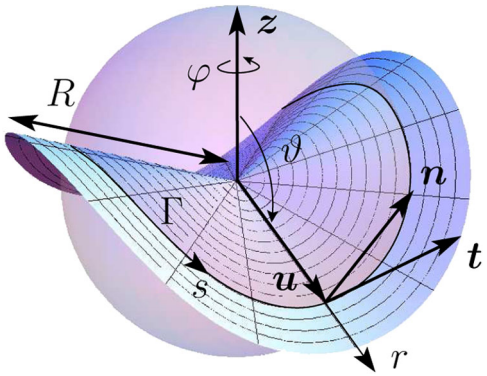

FIG. 1 (color online). Geometry of the e cone with $\varphi_e = \frac{2\pi}{9}$.

vectors form a right-handed surface basis. In the direction of $\boldsymbol{u}$ the surface is flat. The curvature along s is given by $\kappa = -\boldsymbol{n} \cdot \boldsymbol{t}'$. It is easy to show that κ is also the geodesic curvature of Γ on the unit sphere. It should, however, not be mistaken for the Frenet curvature.

Our first task is to identify the configurations that minimize the bending energy of an unstretchable cone of radius R with a surplus angle $\varphi_e > 0$. If we introduce the cutoff r_0 at the apex and integrate over the radial direction, the bending energy is given by $B = (a/2) \oint_\Gamma ds \kappa^2$; the dimensional dependence of B is absorbed into the parameter $a = \ln(R/r_0)$. While it will set the magnitude of the stresses in the cone, it does not play any direct role in determining the shape of the e cone. The constraint of unstretchability is implemented by adding a term to the energy functional which fixes the metric via a set of local Lagrange multipliers T^{ab} [12]. These can be identified with a conserved tangential stress.

The shape equation and its solution.—There is a remarkably simple way to determine the shape of the surface: first recall that to every continuous symmetry of a system a conserved Noether current exists. As the apex of the e cone is fixed, translational invariance is broken. The bending energy is, however, rotationally invariant. The corresponding conserved vector $\boldsymbol{J}$, related to the torque about the apex, is given by [12]

$$\boldsymbol{J}/a = (\kappa^2/2 - C_\parallel)\boldsymbol{n} + \kappa' \boldsymbol{t} + \kappa \boldsymbol{u}. \tag{1}$$

We will suppose that $\boldsymbol{J}$ can be aligned with the $\boldsymbol{z}$ axis, $\boldsymbol{J} = J\boldsymbol{z}$. Its square directly yields the first integral of the shape equation of the surface

$$\tilde{J}^2 - C_\parallel^2 = \kappa'^2 + \kappa^4/4 + (1 - C_\parallel)\kappa^2, \tag{2}$$

where we define $\tilde{J} := J/a$. The constant $C_\parallel$ is associated with the fixed arclength; it will determine the stress established in the surface. Equation (2) is identical to the equation describing the behavior of *planar* Euler elastica with (scaled) tension $\tilde{\sigma} := C_\parallel - 1$ and κ in place of the Frenet curvature. It is completely integrable in terms of elliptic functions [13,14]. The *intrinsic* closure condition $\kappa(s_e) = \kappa(0) = 0$ will provide a "quantization" of the solution: the e cone has to be periodic in equilibrium with a period of s_e/n, where n is the number of folds. Solving Eq. (2) for κ we obtain

$$\kappa(s) = 4\sqrt{-k}\,[\mathcal{K}(k)/S]\ \mathrm{sn}[2s\mathcal{K}(k)/S, k], \tag{3}$$

where $S = s_e/2n$. The function $\mathrm{sn}(s, k)$ is the sine of the Jacobi amplitude $\mathrm{am}(s, k)$ with parameter k. The symbol $\mathcal{K}(k)$ denotes the complete elliptic integral of the first kind [15]. The parameter k is directly related to the stress $C_\parallel$ and the torque $\tilde{J}$.

To obtain the shape, consider the projections of $\boldsymbol{J}$ with respect to the local trihedron. Projecting onto $\boldsymbol{u}$

$$\tilde{J}(\boldsymbol{z} \cdot \boldsymbol{u}) = \tilde{J} \cos\vartheta = \kappa \tag{4}$$

yields the polar angle ϑ as a function of s since $\kappa(s)$ is known. Equation (4) places a strong constraint on the equilibrium shape. In particular, it implies that the only equilibrium shape consistent with a deficit angle is a circular cone. Projecting $\boldsymbol{J}$ onto $\boldsymbol{t}$ reproduces the derivative of Eq. (4). The remaining projection

$$\tilde{J}(\boldsymbol{z} \cdot \boldsymbol{n}) = \tilde{J}\varphi' \sin^2\vartheta = \kappa^2/2 - C_\parallel \tag{5}$$

allows one to determine the azimuthal angle φ via a simple integration.

The closure of the surface in Euclidean space $\mathbb{R}^3$ provides a second (*extrinsic*) closure condition, i.e., $\varphi(s_e) = 2\pi$. This equation identifies the constant k implicitly as a function of the surplus angle φ_e and the quantum number n. Its numerical solution can be approximated remarkably well by a polynomial of third order in φ_e. For small φ_e, we find $k = a_1\varphi_e + \mathcal{O}(\varphi_e^2)$, where $a_1 = -\frac{1}{2\pi}(1 - \frac{1}{n^2})$.

Surface shapes.—The e cone has to have two or more folds. This is a consequence of the four-vertex theorem [16,17]. If the surplus angle is small, one finds a solution with no self-contact for all natural numbers $n \geq 2$. As an example, the first three n folds for $\varphi_e = 2\pi$ are plotted in Figs. 2(b) and 2(d). It is child's play to construct paper models; the twofold illustrated consists of two circular paper discs, each with a radial cut, glued together along the opposite sides of the cut. The model [see Fig. 2(a)] closely resembles the calculated shape even though the surplus angle in question involves deformations of the flat geometry well outside the linear regime.

As φ_e is increased, the conical geometry becomes more crowded and, at some point, the mathematical surface will intersect itself. This happens first with the twofold. The physical surface, of course, will not self-intersect. Where different regions come into contact, they will experience forces and they will deform accordingly [18]. To determine the critical surplus angle $\varphi_e^{\mathrm{kiss}}$ above which this happens, consider the opening angle $\alpha = \vartheta(S/2)$ at the turning point. It is given by $\alpha = \arccos(\tilde{J}^{-1}\kappa_{\max})$ with $\kappa_{\max} = 4\sqrt{-k}\mathcal{K}(k)/S$. When $\alpha = 0$ the two sides of the twofold touch along the $\mathbf{z}$ axis and Eqs. (4) and (5) simplify to $\tilde{J} = \kappa_{\max}$ and $\tilde{J}^2 = 2C_\parallel$. This implies that

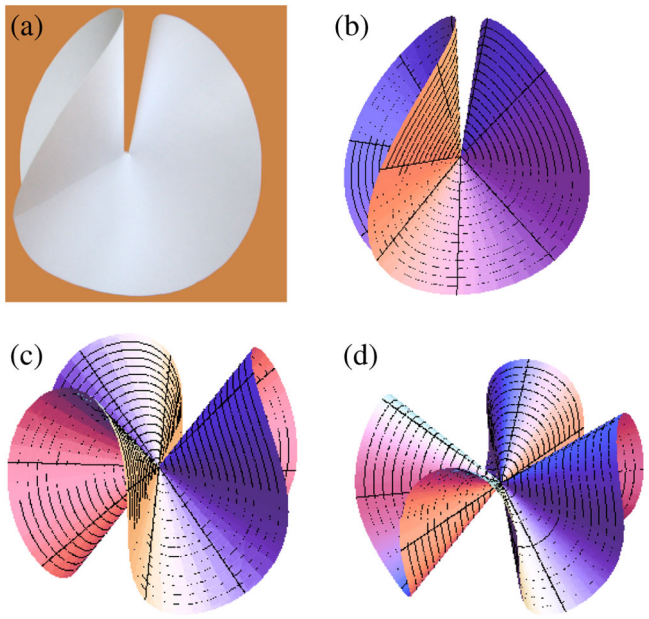

FIG. 2 (color online). Paper model (a) and calculated surface shapes for $\varphi_e = 2\pi$ with $n = 2$ (b), $n = 3$ (c), and $n = 4$ (d).

$S^2 = 4(1-k)\mathcal{K}(k)^2$. Solving this equation together with the extrinsic closure condition numerically yields $k \approx -0.28$ and $\varphi_e^{\text{kiss}} \approx 7.08$. For e cones with more than two folds, the situation is more complicated. Adjacent folds touch pairwise at some nonvanishing opening angle. The corresponding *kissing conditions* are now $\varphi'(s^j_{\text{kiss}}) = 0$ and $\varphi(s^j_{\text{kiss}}) = (2j-1)\pi/2n$, where $j \in \{1, \ldots, 2n\}$. In Table I the values of φ_e^{kiss} of various n folds are given. Interestingly, φ_e^{kiss} converges to $\varphi_{e,\max}^{\text{kiss}} \approx 35.23$ from below if n is sent to infinity. This implies that one cannot find a stable surface with $\varphi_e > \varphi_{e,\max}^{\text{kiss}}$ which does not make contact with itself. The detailed analysis of these touching geometries lies beyond the scope of this Letter. The twofold, however, is straightforward to study since it will touch itself only at two segments of the unit circle of arclength φ_t each. Using the kissing conditions with $n = 2$, φ_t and $C_\parallel$ can be determined simultaneously for any given φ_e.

Stresses in the e cone.—Even though there are no external forces acting on the cone, stresses will be set up in the surface due to bending as well as the constraint on the metric. The stress tensor T^{ab} which fixes the latter is purely tangential. It is diagonal with respect to the basis $(\boldsymbol{u}, \boldsymbol{t})$ and constant along curves of constant radial distance r. Its nonvanishing components along $\boldsymbol{t}$ and $\boldsymbol{u}$ are given by $T_\parallel = -C_\parallel/r^2$ and, for a large disc, $T_\perp = -T_\parallel$ [12]; it is nonisotropic.

TABLE I. Kissing points for different n folds.

n	2	3	4	5	10	50	$\to \infty$
φ_e^{kiss}	7.08	13.30	17.78	21.12	29.38	34.92	35.23

In Fig. 3 $C_\parallel$ is plotted as a function of φ_e for different values of n. For small values of φ_e the expansion $k \approx a_1\varphi_e$ can be used to write $C_\parallel = (1-n^2) - (4\pi)^{-1} \times (3-7n^2)\varphi_e + \mathcal{O}(\varphi_e^2)$. In this regime the stress $C_\parallel$ is negative; this corresponds to a compressive stress along the tangential direction; an equal compensating tensile stress will act radially. $C_\parallel$ is nonvanishing when $\varphi_e = 0$, representing the critical compression necessary to buckle the planar sheet into the corresponding mode. For a fixed surplus angle the absolute value of $C_\parallel$ increases with n. If φ_e is increased, the curves for different n converge and appear to intersect in a single point (the twofold is exceptional making contact with itself before this point is reached). Investigated more carefully, however, a set of adjacent intersection points is found which converge to $\varphi_e \approx 7.47$ for $n \to \infty$. Above this region each curve reaches a maximum which diverges quadratically with n. If $n > 5$ and φ_e sufficiently large, $C_\parallel$ is greater than 1. This implies that the tension $\tilde{\sigma}$ in the corresponding planar Euler elastica changes sign [cf. text below Eq. (2)].

However, one must remember that the full stress in the e cone includes a contribution due to bending. This becomes increasingly important as φ_e gets larger. The tangential projection $\boldsymbol{f}_\parallel$ of the *full* stress tensor can be written as $\boldsymbol{f}_\parallel = (\tilde{J}/r^2)\sin\vartheta\boldsymbol{\varphi}$, where $\boldsymbol{\varphi}$ is the basis vector of φ. The transmitted force per length along Γ is a maximum at the equator and a minimum at the turning points. It always points in the direction of $\boldsymbol{\varphi}$; the tangential part of $\boldsymbol{f}_\parallel$ becomes tensile where φ' is negative. These results can easily be verified by cutting the paper model along the flat direction and observing how the sheet reacts.

Bending energy.—We are also able to obtain an analytical expression for the bending energy $\tilde{B} := B/(as_e/2)$ using the expression for κ in terms of elliptic functions: $\tilde{B} = 64\mathcal{K}(k)[\mathcal{E}(k) - \mathcal{K}(k)](n/s_e)^2$. We have normalized the bending energy by dividing by the area of the e cone.

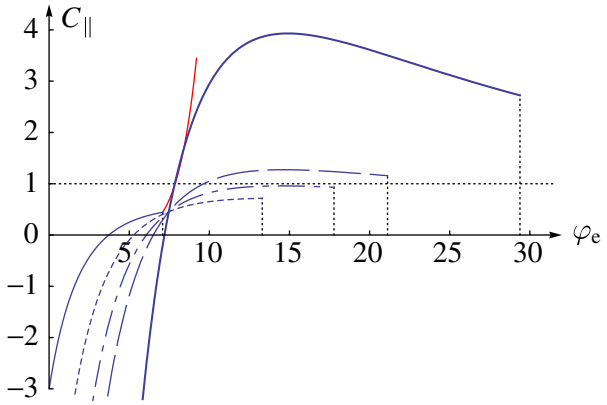

FIG. 3 (color online). Stress $C_\parallel$ as a function of φ_e for $n = 2$ (solid line), 3 (short-dashed), 4 (dash-dotted), 5 (long dashed), and 10 (bold solid). The red curve shows $C_\parallel$ for the touching twofold. Above $C_\parallel = 1$ the tension $\tilde{\sigma}$ along the curve Γ changes sign.

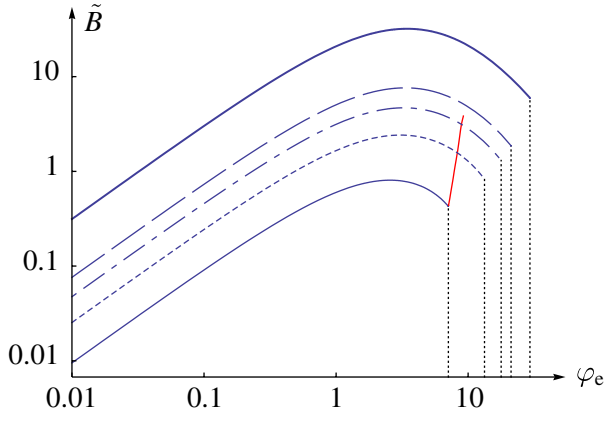

FIG. 4 (color online). Scaled bending energy $\tilde{B}$ for $n = 2$ (solid line), 3 (short-dashed), 4 (dash-dotted), 5 (long dashed), and 10 (bold solid). The red curve shows $\tilde{B}$ for the touching twofold.

The function $\mathcal{E}(k)$ is the complete elliptic integral of the second kind [15].

For fixed φ_e, $\tilde{B}$ scales essentially with n^2 since k depends only weakly on n. In Fig. 4 the energy is plotted as a function of φ_e for the lowest n folds. For small φ_e, all curves behave as $\tilde{B} \approx \frac{1}{\pi}(n^2 - 1)\varphi_e$. The twofold is the ground state if φ_e is below the critical value associated with self-intersection. This observation is confirmed nicely by the paper model [see Fig. 2(a)]. For higher values of φ_e one needs to examine the folding pattern that is consistent with self-contact. Initially, by continuity, it will remain the ground state. However, with increased crowding one begins to force up the average curvature: above $\varphi_e = 8.27$ the threefold possesses lower energy than the touching symmetrical twofold and the e cone may flip from $n = 2$ to $n = 3$. Equivalent behavior is expected if φ_e is increased. To analyze the stability of our solutions, it is necessary to examine the second variation $\delta^2 H$ of the total energy functional. This is complicated by the fact that the local constraint of isometry has to be imposed on the deformations about the conical background. What is remarkable is that the calculation is tractable. One can show that $\delta^2 H$ is of the form $\oint ds \phi \mathcal{L} \phi$, where $\phi = \boldsymbol{n} \cdot \delta \boldsymbol{X}$ denotes the normal deformation of the surface. The relic of the isometry constraint is that $\oint \kappa \phi = 0$. The operator $\mathcal{L} = \partial_s^4 + \frac{1}{2}\partial_s V_1 \partial_s + \frac{1}{2}(V_2 + \frac{1}{2}V_1'')$ is self-adjoint and of fourth order in ∂_s. The potentials V_1 and V_2 are functions of κ and its derivatives. Using a decomposition of ϕ into Fourier modes, one can determine the eigenvalues of $\mathcal{L}$ for arbitrary φ_e and n. They are all positive; e cones free of self-contacts are stable.

Conclusions.—We have described the equilibrium states of a cone exhibiting a surplus angle. If we suppose that growth is slow compared to any viscoelastic time scale, the surface finds its equilibrium and the approach we have presented describes the evolution of the shape of a growing conical tissue. If the circumferential arclength increases linearly with the geodesic radius, the surplus angle will remain constant; the cone will scale as it grows. Another mode of growth involves an increasing surplus angle. An initially flat disc will develop into a twofold, although a fluctuation may favor some higher energy state which we have seen is stable. However, if at some point, the surplus angle reaches $\varphi_e^{\text{kiss}}(2)$ the surface will make contact which is costly energetically. At some higher value one would expect the surface to flip spontaneously into a threefold. This will continue through a fourfold and so fifth with increasingly higher speed. Above $\varphi_{e,\max}^{\text{kiss}}$, however, self-contact becomes unavoidable. Internal local pressure will build up as the spherical volume occupied by the cone is packed more and more densely.

What we have learned about the e cone lays the foundation for understanding more general morphologies. If a disc surrounding the apex is removed, the cone can relax into some other flat geometry. Indeed one can easily verify with a paper model that the $n = 2$ ground state is unstable with respect to such deformations. These truncated cones can also be glued together to model surfaces which are not flat: a surface of constant negative Gaussian curvature can be approximated by a telescope formed by such annuli.

Partial support from CONACyT grant 51111 as well as DGAPA PAPIIT grant IN119206-3 is acknowledged. The authors would like to thank A. Boudaoud, L. Boué, and P. Vázquez for helpful discussions.

[1] R. A. L. Jones, *Soft Condensed Matter* (Oxford University Press, New York, 2002).
[2] M. Rubinstein and R. H. Colby, *Polymer Physics* (Oxford University Press, New York, 2003).
[3] W. Helfrich, Z. Naturforsch. **28c**, 693 (1973).
[4] U. Seifert, Adv. Phys. **46**, 13 (1997).
[5] T. A. Witten, Rev. Mod. Phys. **79**, 643 (2007).
[6] Y. Klein *et al.*, Science **315**, 1116 (2007).
[7] J. Dervaux and M. Ben Amar, Phys. Rev. Lett. **101**, 068101 (2008).
[8] A. Lobhovsky *et al.*, Science **270**, 1482 (1995).
[9] M. Ben Amar and Y. Pomeau, Proc. R. Soc. A **453**, 729 (1997).
[10] E. Cerda and L. Mahadevan, Phys. Rev. Lett. **80**, 2358 (1998).
[11] K. A. Serikawa and D. F. Mandoli, Planta **207**, 96 (1998).
[12] J. Guven and M. M. Müller, J. Phys. A **41**, 055203 (2008).
[13] J. Langer and D. A. Singer, J. Diff. Geom. **20**, 1 (1984).
[14] J. Arroyo *et al.*, J. Phys. A **39**, 2307 (2006).
[15] *Handbook of Mathematical Functions*, edited by M. Abramowitz and I. A. Stegun (Dover, New York, 1970), 9th ed.
[16] D. Fuchs and S. Tabachnikov, *Mathematical Omnibus: Thirty Lectures on Classic Mathematics* (American Mathematical Society, Providence, 2007).
[17] J. J. Nuño Ballesteros and M. C. Romero Fuster, J. Geom. Phys. **46**, 119 (1993).
[18] L. Boué *et al.*, Phys. Rev. Lett. **97**, 166104 (2006).